**Atmospheric
Chemistry
and Physics**

Spatiotemporal variations of ambient PM_{10} source contributions in Beijing in 2004 using positive matrix factorization

S. D. Xie[1], Z. Liu[1], T. Chen[2], and L. Hua[2]

[1]College of Environmental Sciences and Engineering, State Key Joint Laboratory of Environmental Simulation and Pollution Control, Peking University, Beijing 100871, People's Republic of China
[2]Beijing Municipal Environmental Monitoring Center, Beijing 100044, People's Republic of China

Abstract. Source contributions to ambient PM_{10} (particles with an aerodynamic diameter of $10\,\mu$m or less) in Beijing, China were determined with positive matrix factorization (PMF) based on ambient PM_{10} composition data including concentrations of organic carbon (OC), elemental carbon (EC), ions and metal elements, which were simultaneously obtained at six sites through January, April, July and October in 2004. Results from PMF indicated that seven major sources of ambient PM_{10} were urban fugitive dust, crustal soil, coal combustion, secondary sulfate, secondary nitrate, biomass burning with municipal incineration, and vehicle emission, respectively. In paticular, urban fugitive dust and crustal soil as two types of dust sources with similar chemical characteristics were differentiated by PMF. Urban fugitive dust contributed the most, accounting for 34.4% of total PM_{10} mass on an annual basis, with relatively high contributions in all four months, and even covered 50% in April. It also showed higher contributions in southwestern and southeastern areas than in central urban areas. Coal combustion was found to be the primary contributor in January, showing higher contributions in urban areas than in suburban areas with seasonal variation peaking in winter, which accounted for 15.5% of the annual average PM_{10} concentration. Secondary sulfate and secondary nitrate combined as the largest contributor to PM_{10} in July and October, with strong seasonal variation peaking in summer, accounting for 38.8% and 31.5% of the total PM_{10} mass in July and October, respectively. Biomass burning with municipal incineration contributions were found in all four months and accounted for 9.8% of the annual average PM_{10} mass concentration, with obviously higher contribution in October than in other months. Incineration sources were probably located in southwestern Beijing. Contribution from vehicle emission accounted for 5.0% and exhibited no significant seasonal variation. In sum, PM_{10} source contributions in Beijing showed not only significant seasonal variations but also spatial differences.

1 Introduction

According to the Report on the State of the Environment in China issued by State Environmental Protection Administration (SEPA), from 2003 through 2006, there were 54.4%, 53.2%, 48.1% and 43.4% of Chinese cities where annual average daily concentration of PM_{10} (inhaled particulate matter, particles with an aerodynamic diameter of $10\,\mu$m or less) exceeded the level II of National Ambient Air Quality Standard $100\,\mu$g m^{-3} (State Environmental Protection Administration (SEPA), 2005, 2007). PM_{10} has become the primary air pollutant in cities of China. Therefore, source apportionment studies are of great significance for controlling ambient PM_{10} pollution in China.

Research on sources of ambient particulate matter began with analyzing source emission inventories and using dispersion models based on them. The focus shifted from source to receptor in the 1970s. Receptor models identify and apportion sources by analyzing aerosol chemical compositions and physical parameters at a sampling site (or receptor) without information about source strengths, do not rely on meteorological data, and can identify fugitive emission sources. With such advantages, receptor models have been developing fast from its birth. Based on whether source profiles should be known at first, receptor models can be divided into two categories: chemical mass balance model (CMB) and various forms of multivariate statistical models.

Wang (1985) performed the earliest source apportionment study for ambient aerosols in Beijing using factor analysis. Recently, Okuda et al. (2004) performed a CMB study with daily concentrations of trace metals and ionic constituents in aerosols in Beijing from 2001 through 2003, and identified crustal soil and coal combustion as two primary sources. Dan et al. (2004) identified PM$_{2.5}$ sources in Beijing by comparing concentrations of OC, EC and trace elements at receptor sites. Zheng et al. (2005) determined 9 sources of PM$_{2.5}$ in Beijing using CMB model with particle-phase organic compounds as fitting tracers. Bi et al. (2005) performed a CMB source apportionment of ambient PM$_{10}$ in six cities in northern China based on measured chemical profiles of local resuspended dust and coal combustion emission, and found resuspended dust and coal fly ash to be the primary PM$_{10}$ sources. However, it is difficult to establish databases of specific local source profiles for CMB studies. Furthermore, similarities among some source profiles may easily cause problems of collinearity. The CMB studies above used a variety of source categories and profiles which led to the poor comparability of their results, due to the incomplete information on local source profiles.

Therefore, multivariate statistical methods have been used more extensively for source apportionment of ambient particles in China in recent years. Sun et al. (2004) performed a factor analysis for a preliminary discussion of ambient PM$_{10}$ sources in Beijing. Wang et al. (2005) used Ca^{2+}/Al ratio to estimate the mixing of different dust sources and roughly calculated PM$_{2.5}$ source contributions by factor analysis. But these traditional statistical methods could not identify sources elaborately and precisely.

A new approach named positive matrix factorization (PMF) developed by Paatero and Tapper (1994, 1997) takes an explicit least squares approach by integrating non-negative constrains into the optimization process and utilizing the error estimates for each data value as point-by-point weights. Due to the advantages over traditional factor analysis methods, during the last one or two decades, PMF was successfully used in source apportionment of airborne particulate matter in the United States (Kim and Hopke, 2006), Switzerland (Lanz et al., 2007), Spain (Zabalza et al., 2006), Mexico (Johnson et al., 2006), Canada (Lee et al., 2003), Korea (Han et al., 2005), as well as in China (Lee et al., 1999; Yuan et al., 2006; Song et al., 2006, 2007). Most recently, Reff et al. (2007) reviewed the methods for using PMF model, and recommended future publications to fully document procedures for data preparation, PMF application, and result interpretation.

Since December 1998, a series of measures have been taken to control pollution of SO$_2$, NO$_x$ and PM$_{10}$ in Beijing. However, compared with the significant decline of SO$_2$ concentration, from 80 μg m^{-3} in 1999 to 53 μg m^{-3}, ambient PM$_{10}$ mass concentration remained at a high level. From 1999 to 2006, annual average PM$_{10}$ mass concentrations were respectively 180, 162, 165, 166, 141, 149,

142 and 161 μg m^{-3} (Beijing Environmental Protection Bureau, 2004, 2005, 2006), which were about 65% higher than National Ambient Air Quality Standard (level II) of 100 μg m^{-3}. These concentrations were also more than two times of those in magacities as New York, London, and Moscow. Previous control measures showed no significant effects at all, due to the complexity of PM$_{10}$ sources in Beijing. With such background, we performed a source apportionment study using PMF model for ambient PM$_{10}$ in Beijing in 2004, in order to provide scientific basis for controlling PM$_{10}$ pollution more effectively.

2 Methods

2.1 Sampling and chemical analysis

Six PM$_{10}$ sampling sites were set up at Ming Tombs (MT), Chegongzhuang (CGZ), Gucheng (GC), Fangshan (FS), Yizhuang (YZ), and National Olympic Sports Center (AT) (Chen et al., 2006), as shown in Fig. 1. Ming Tombs (MT) site located in Changping District and 45 km northeast from central Beijing is currently a background air quality monitoring site for Beijing Environmental Monitoring Network. Chegongzhuang (CGZ) site near Chegongzhuang East Road and National Olympic Sports Center (AT) site next to the Northern 4th ring road are two traffic sites representing different streets in urban areas. Yizhuang (YZ) as suburban site near the Southern 5th Ring Road with Beijing's southeastern industrial emission sources on its north is a typical representation for economic development area. It is also located on the aerosol transport path in southeastern Beijing. Gucheng (GC) site, an industrial site, is located next to the Capital Iron and Steel Plant in western Beijing. Fangshan (FS), located in southwestern Beijing and surrounded by Beijing Yanshan Petrochemical Corporation as well as several building material plants producing cement, lime, and sandstones, is a typical representation of centralized area by petrochemical and building material industries. It is also a representative site on the southwestern aerosol transport path.

PM$_{10}$ samples were collected using TH-16A Medium-Volume Samplers made by Wuhan Tianhong Intelligence Instrumentation Facility simultaneously at these six sites on the middle ten days in January, April, July and October in 2004 with sampling duration of 23 h and 30 min on each sampling day, from 09:00 a.m. to the next 08:30 a.m. Quartz fiber filters were used for analysis of organic carbon (OC), elemental carbon (EC), and Teflon filters were used for analysis of PM$_{10}$ mass concentration, elements and ions concentrations. Gravimetric method was used to determine PM$_{10}$ mass concentration. Inductively coupled plasma mass spectrometry (ICP-MS), graphite furnace atomic absorption spectrometry (GF-AAS), hydrogenation atomic fluorescent spectrometry (HG-AFS) were used to determine concentrations of 20 elements: Al, As, Ba, Ca, Cd, Cr, Cu, Fe, K, Mg,
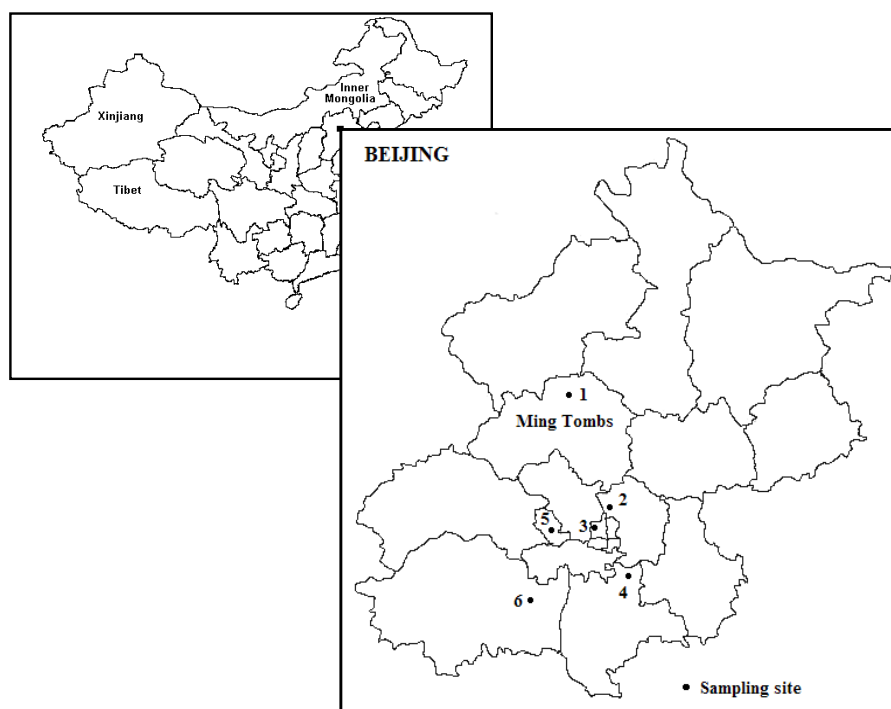
Fig. 1. Locations of the sampling sites in Beijing 1. Ming Tombs (MT) 2. National Olympic Sports Center (AT) 3. Chegongzhuang (CGZ) 4. Yizhuang (YZ) 5.Gucheng (GC) 6. Fangshan (FS).

Mn, Na, Ni, Pb, Sc, Se, Si, Ti, V, and Zn. Ion Chromatography (IC) (Dionex, Model DX-500) was used for analyzing NH$_4^+$, NO$_3^-$, and SO$_4^{2-}$ concentrations. Organic carbon (OC) and elemental carbon (EC) were measured using a thermal/optical carbon analyzer produced by Sunset Laboratory Inc., USA. In total, 243 PM$_{10}$ samples were collected at the six sites, for whom concentrations of PM$_{10}$ species mentioned above were measured.

2.2 Source apportionment by positive matrix factorization

2.2.1 Positive matrix factorization (PMF) model

Positive matrix factorization (PMF, Paatero and Tapper, 1994, Paatero, 1997) is an advanced factor analysis technique that uses non-negativity constraints and allows non-orthogonal factors. The bilinear factor analytic model denoted as PMF2 can be written as,

$$\mathbf{X} = \mathbf{GF} + \mathbf{E} \tag{1}$$

where $\mathbf{X}$ is the $\mathbf{n} \times \mathbf{m}$ matrix of species concentrations in ambient PM$_{10}$; G is the $\mathbf{n} \times \mathbf{p}$ matrix of source contributions; $\mathbf{F}$ is the $\mathbf{p} \times \mathbf{m}$ matrix of source profiles, and the residual matrix $\mathbf{E}$ is defined as the difference between the observed concentration $\mathbf{X}$ and the modeled values, $\mathbf{Y}$:

$$e_{ij} = x_{ij} - y_{ij} = x_{ij} - \sum_{k=1}^{p} g_{ik} f_{kj} \tag{2}$$

where $i=1, ..., n$ samples; $j=1, ..., m$ species; $k=1, ..., p$ sources. The model uses least-squares fit of the data to minimize the objective function, $Q(E)$, which is defined as

$$Q(E) = \sum_{i=j}^{m} \sum_{j=1}^{m} (e_{ij}/\sigma_{ij})^2 \tag{3}$$

where σ_{ij} is the standard deviation corresponding to the observed value x_{ij}.

PMF was run in the robust mode, in order to decrease the impact of extreme values or outliers that are very common in environmental data (Paatero, 2004).

2.2.2 Data pretreatment

Missing concentration values and below detection limit (BDL) values were treated with the methods by Polissar et al. (1998): missing concentration values were replaced by the arithmetic mean concentration of that species and four times of this mean value were assigned as the corresponding uncertainties. BDL values were replaced by half of the detection limit (DL_j) for that species and the corresponding uncertainties were estimated as in Eq. (4). The uncertainties for determined values were estimated by the following Eqs. (5) and (6) (Jon Zabalza et al., 2006):

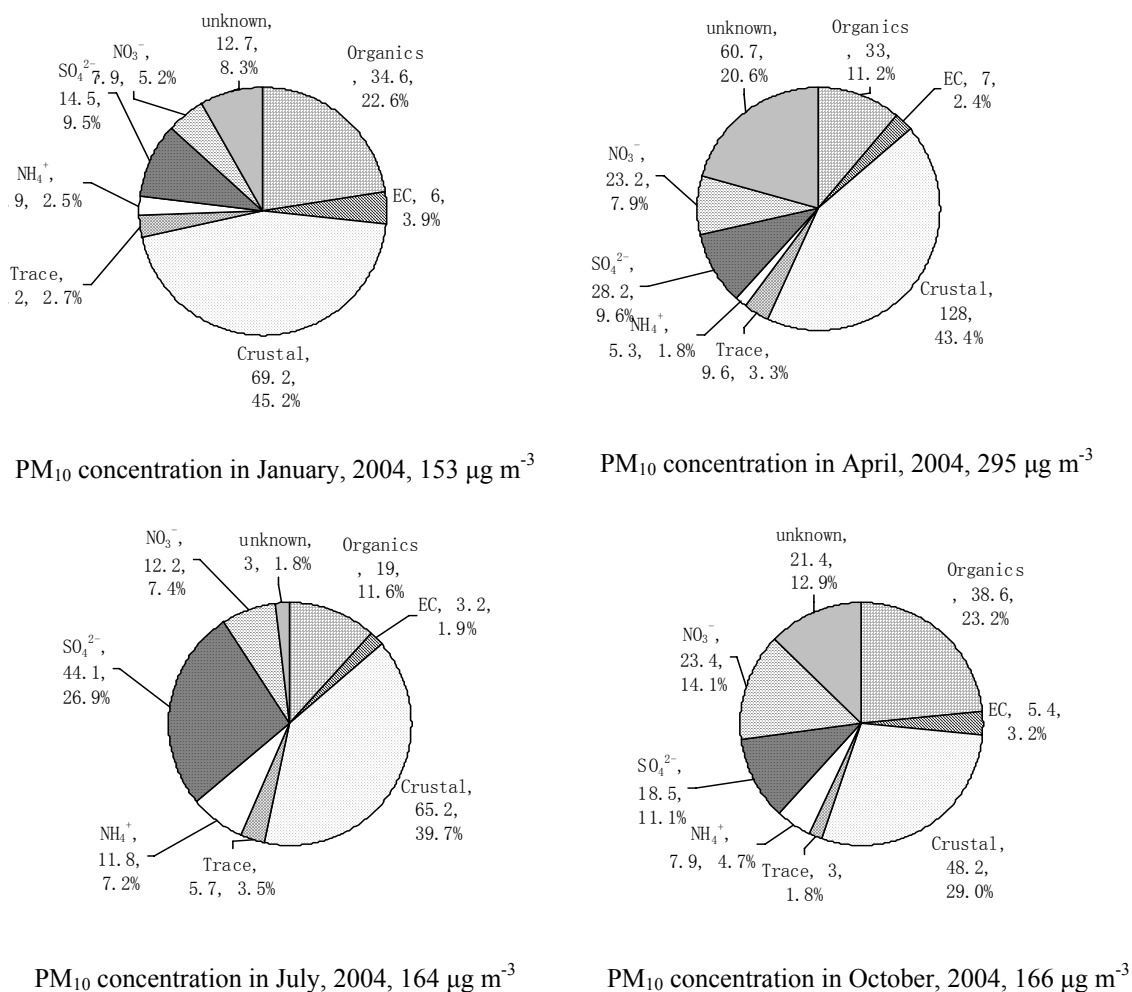$$\sigma(x_{ij} < DL_j) = x_{ij} + \frac{2}{3}DL_j \tag{4}$$

PM$_{10}$ concentration in January, 2004, 153 μg m^{-3}

PM$_{10}$ concentration in April, 2004, 295 μg m^{-3}

PM$_{10}$ concentration in July, 2004, 164 μg m^{-3}

PM$_{10}$ concentration in October, 2004, 166 μg m^{-3}

Fig. 2. Proportional ambient PM$_{10}$ chemical compositions in Beijing in January, April, July and October, 2004.

$$\sigma(DL_j < X_{ij} < 3DL_j) = 0.2x_{ij} + \frac{2}{3}DL_j \qquad (5)$$

$$\sigma(x_{ij} > 3DL_j) = 0.1x_{ij} + \frac{2}{3}DL_j \qquad (6)$$

In this study, Sc was not included in PMF analysis due to its large number of BDL valus.

2.2.3 Model trial

The first step in PMF analysis is to determine the number of factors and identify the related sources. Then the chemical composition profiles for the sources and their contributions to each sample are acquired from the **F** and **G** matrices in PMF output, respectively. In order to choose the factor numbers, all the possibilities should be compared to find the most reasonable solution. In this process, mathematical diagnostics in PMF output are used to examine the technical feasibilities. In this study, the diagnostics taken into considered included the value of Q, which should be proximated by the

number of data points; frequency distribution of scaled residuals (e_{ij}/σ_{ij}), most of which should be between -2 and $+2$ to guarantee a nice agreement between the results and the input data; rotmat, a matrix generated by the PMF model to estimate the rotational ambiguities of the factors; and the coefficients in the multiple linear regression (see Eq. 7), which should be all positive (Lee et al., 1999). The solusions with 6, 7, 8, 9 factors in our study were found to be relatively reasonable after 2–12 factors were examined carefully. Meanwhile, since these mathematical parameters cannot guarantee the interpretability of the solution, further examination based on the preliminary recogonitions for the pollution sources in the target area is necessary to assure the final solution representing the local conditions of the atmospheric pollution. By referring to our previous understanding of pollution sources in Beijing and other findings on identificaion of PMF factors (e.g. Zabalza et al., 2006; Lee and Hopke, 2006; Lee et al., 1999), we chose a 7-factor solution as the best. The second step is to control rotation and optimize the solution, using the
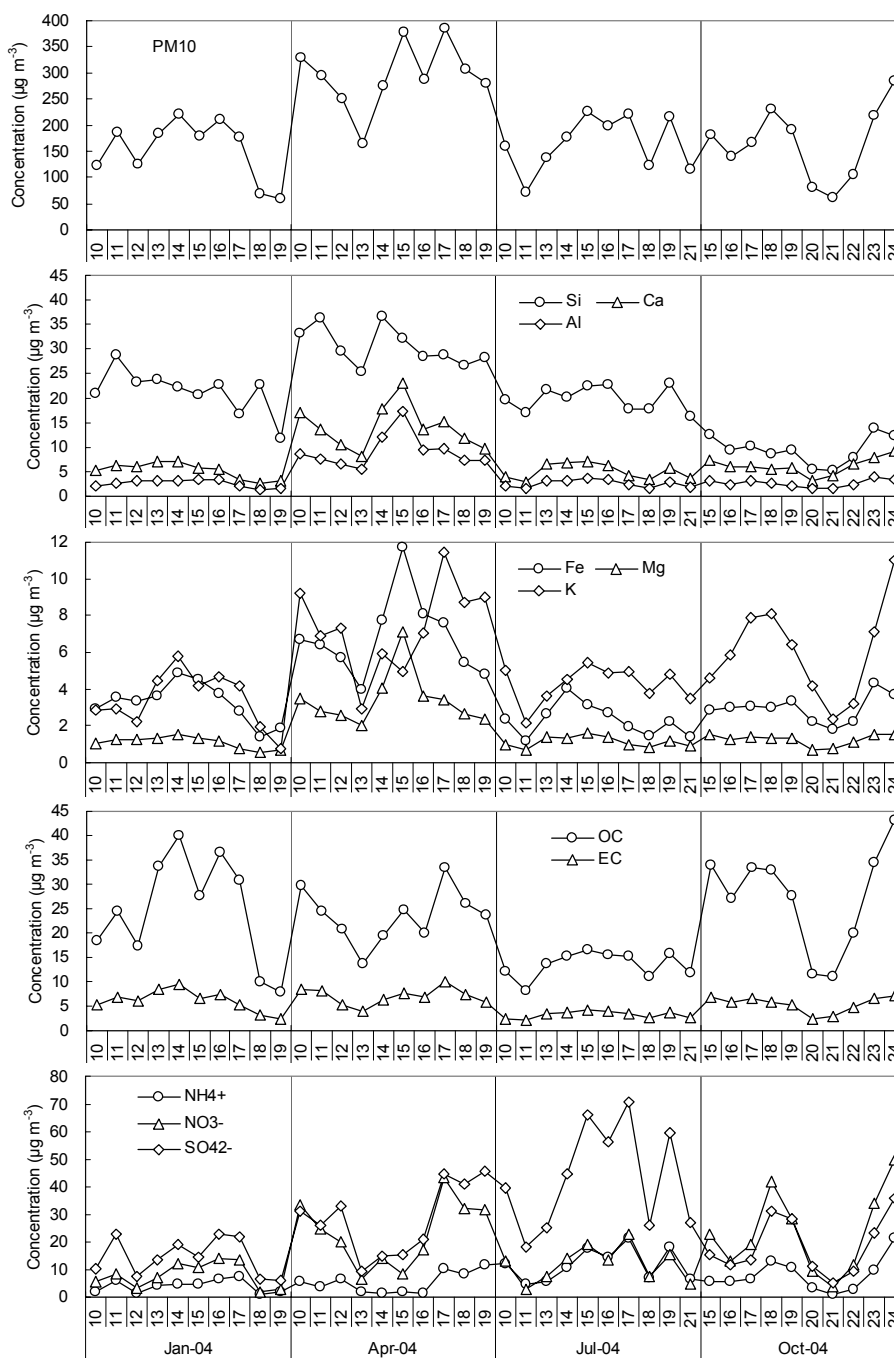
Fig. 3. Average daily variations for concentrations of PM$_{10}$, Si, Al, Ca, Fe, Mg, K, OC, EC, SO$_4^{2-}$, NO$_3^-$, NH$_4^+$ in 2004 Fig. 4. PMF resolved source profiles for ambient PM$_{10}$ in Beijing.

parameters FPEAK and *FKEY* (or *GKEY*) provided by the model (Paatero, 2004). Usually PMF is run with different FPEAK values to find the range within which the objective function Q does not show a significant change. The optimal solution should lie in this range (Paatero et al., 2002). Sometimes, the unrealistic concentration values in resolved sources can be pulled down toward zero to obtain a reasonable profile through the matrix **FKEY**.

After numerous runs, FPEAK=0 and a **FKEY** matrix provided the most physically reasonable solution. In the **FKEY** matrix, values of all elements were set to 0 except for values of 3 and 5 for OC and EC in secondary nitrate; and values of 5, 3, 5, and 5 for SO$_4^{2-}$ in biomass burning, crustal soil, secondary nitrate, and vehicle emission, respectively.

The results of PMF analysis were scaled to the measured concentration using a scaling constant s_k, obtained by

regressing the measured total PM_{10} mass against the factor scores, g_{ik}, determined by the model (Hopke et al., 1980), as described by Eq. (7) below,

$$x_{ij} = \sum_{k=1}^{p} (s_k g_{ik})(f_{kj}/s_k). \tag{7}$$

3 Results and discussion

3.1 Concentration and chemical composition of ambient PM_{10} in Beijing in 2004

The overall average PM_{10} concentration of the 243 samples at the six sites through the sampling duration was $194 \, \mu g \, m^{-3}$. Average PM_{10} concentrations for January, April, July and October were $153 \, \mu g \, m^{-3}$, $295 \, \mu g \, m^{-3}$, $164 \, \mu g \, m^{-3}$ and $166 \, \mu g \, m^{-3}$, respectively. The highest PM_{10} concentration $482 \, \mu g \, m^{-3}$ appeared on 15 April at FS and the lowest concentration $33.8 \, \mu g \, m^{-3}$ was on October 21 at MT. Average PM_{10} mass concentrations at each site were $231 \, \mu g \, m^{-3}$ at FS, $227 \, \mu g \, m^{-3}$ at GC, $204 \, \mu g \, m^{-3}$ at YZ, $197 \, \mu g \, m^{-3}$ at CGZ, $195 \, \mu g \, m^{-3}$ at AT and $146 \, \mu g \, m^{-3}$ at MT, respectively, indicating that PM_{10} concentration was growing higher from northern Beijing to the south.

Based on the method by Christoforou et al. (2000): (1) concentrations of organics in PM_{10} were obtained from OC concentrations multiplied by 1.4; (2) total concentrations of crustal elements were obtained from sum of Al, Si, Ca, Fe, Ti, Mn, and K oxides concentrations; (3) total concentrations of trace elements were calculated from the sum of As, Cd, Cr, Cu, Mg, Na, Ni, Pb, Se, V, and Zn concentrations. And then the monthly averages of PM_{10} chemical compositions in Beijing in January, April, July, and October, 2004 shown in Fig. 2 were obtained. As seen in Fig. 2, the major chemical components of ambient PM_{10} in Beijing were crustal elements, organics, SO_4^{2-} and NO_3^-, accounting for 39.9%, 16.1%, 13.5% and 8.6% of total PM_{10} mass, respectively. Figure 2 also indicates significant seasonal variations for PM_{10} chemical compositions.

Crustal elements accounted for more than 40% of PM_{10} mass concentration in January, April, and July. SO_4^{2-} in July and NO_3^- in October accounted for 26.9% and 14.1% of PM_{10} mass concentrations in the corresponding months, which were obviously higher than in other months.

Daily concentrations of PM_{10} and its organic and inorganic species in Beijng in 2004 were obtained by averaging the concentration values at the six sites. Figure 3 presents the seasonally different daily variation patterns for each species, with high PM_{10} concentration all through the year. Apart from K, other crustal elements Si, Ca, Al, Fe, and Mg displayed a common pattern, similar as that of PM_{10} mass, which indicated their same source and the domination in PM_{10} concentrations. Especially, daily PM_{10} concentrations in April were almost all comprised of crustal elements. K

and OC concentrations in October stayed high with similar patterns, indicating their same sources, such as biomass burning. OC corresponded with high concentrations in January, April, and October with great daily fluctuations, while EC displayed little monthly variations. The characteristics for SO_4^{2-}, NO_3^- and NH_4^+ variations included high SO_4^{2-} in July and high NO_3^- in October. In addition, NO_3^- concentrations being quite close to NH_4^+ in July allowed us to estimate NH_4NO_3 to be the major form of nitrate; while NO_3^- being obviously higher than NH_4^+ in other months, indicating other forms of nitrate to exist in the particles.

In general, these comparisons above showed that in January PM_{10} were dominated by crustal elements and OC, in April crustal elements, in July SO_4^{2-} and crustal elements, and in October OC, K, and NO_3^-.

3.2 Source identification for ambient PM_{10} in Beijing in 2004

Seven sources of ambient PM_{10} in Beijing were resolved by PMF, which were urban fugitive dust, crustal soil, coal combustion, secondary sulfate, secondary nitrate, biomass burning with municipal incineration, and vehicle emission, for which source profiles were shown in Fig. 4.

The first source profile illustrated in Fig. 4a was characterized by high concentrations of crustal elements, such as Si, Ca, Al, Fe, Mg, Mn and Ti, along with relatively high loadings of OC, EC, SO_4^{2-} and NO_3^-, presenting significant characteristics of urban fugitive dust (Song et al., 2006). This source profile was displayed together with other three types of measured dust profiles in Beijing, namely, urban suspended dust, road dust and construction dust (Hua et al., 2006) in Fig. 5. It can be seen by comparing the chemical profiles in Fig. 5 that concentrations of crustal elements, such as Si, Ca, Al, Fe, Mg, Ti and OC, NO_3^- were comparable in these four dust profiles, while PMF resolved dust profile exhibited higher loadings of SO_4^{2-}, EC and lower loadings of K and Na than other three types of measured dust profiles. These differences might be caused by factor rotations and similar phenomenon has been reported by Lee and Hopke (2006). The abundance of EC, OC and NO_3^- might be due to unavoidable influences from human activities, such as deterioration of waste and deposition of fly ashes from coal combustion. Therefore, this source represented fugitive emission of dust mainly from local roads traffic, agricultural tilling operations, aggregate storage piles, construction operations and was identified as "urban fugitive dust".

The second source profile illustrated in Fig. 4b was one of the most stable factors during model trial, represented by high concentrations of crustal elements Si, Al, Ca, Fe, Mg with relatively high concentration of SO_4^{2-}, showing similar pattern with urban fugitive dust. But the concentration values in this source differed from those in urban fugitive dust. OC and EC were not found in this source and Ca
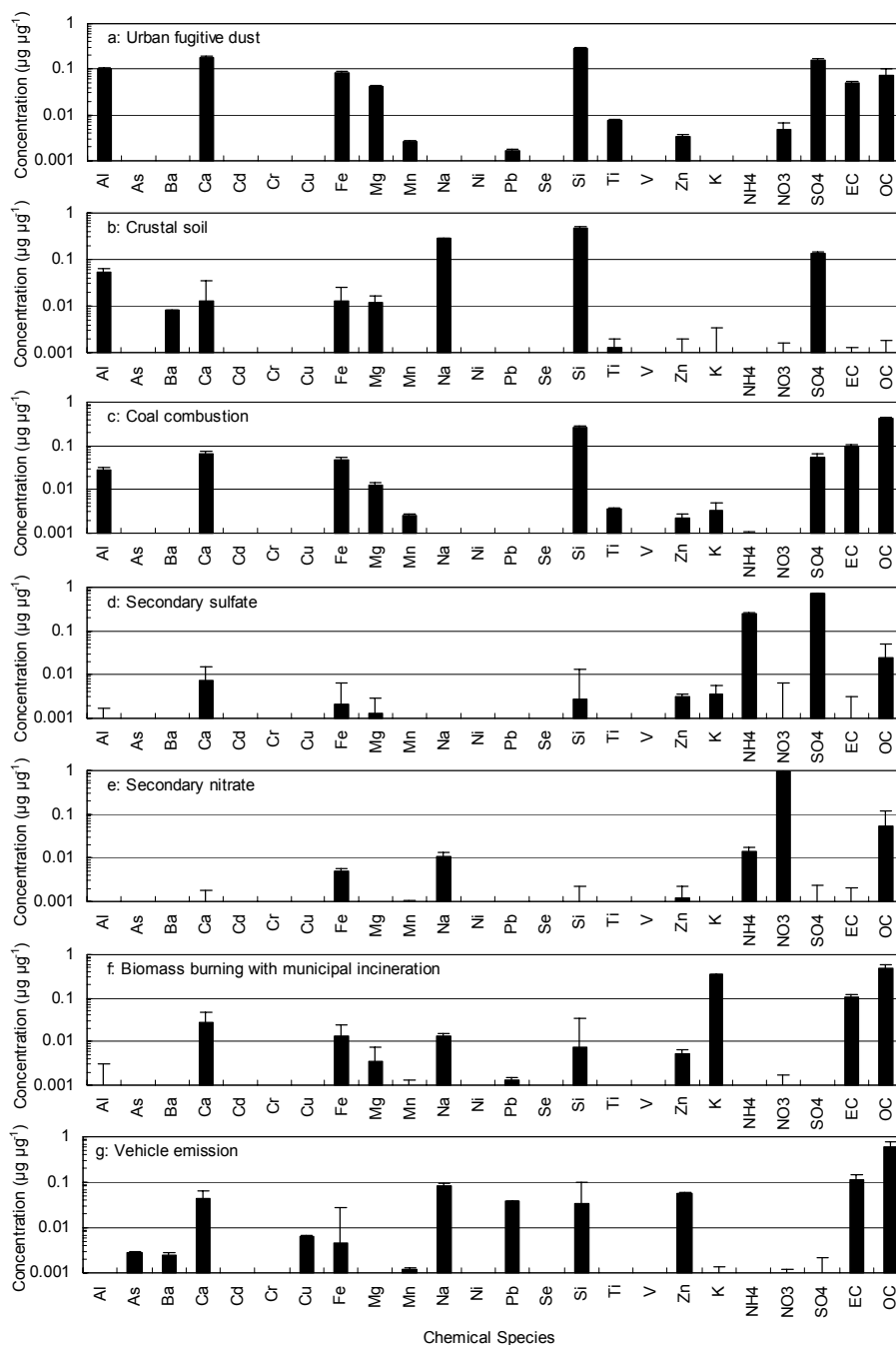
Fig. 4. PMF resolved source profiles for ambient PM$_{10}$ in Beijing.

concentration was lower than in urban fugitive dust, indicating fewer influences by human activities. High SO$_4^{2-}$ concentration in this source might be metal sulfates (e.g. CaSO$_4$ and MgSO$_4$) formed through atmospheric reactions between airborne H$_2$SO$_4$/SO$_2$ and crustal elements (Lee et al., 1999). By all appearances, this source was identified as crustal soil.

PMF successfully indentified these two types of dust source with similar chemical characteristics in Beijing.

The third source profile was presented in Fig. 4c. The major chemical species of this source were Si, Ca, Fe, Al, Mg, Ti, Mn and Zn with high concentrations of OC, EC and SO$_4^{2-}$, revealing the main chemical composition with crustal elements and C. This is the typical pattern for emission from coal combustion (Song et al., 2006 and 2007).

The fourth source profile shown in Fig. 4d was characterized by high concentrations of SO$_4^{2-}$ and NH$_4^+$, along with
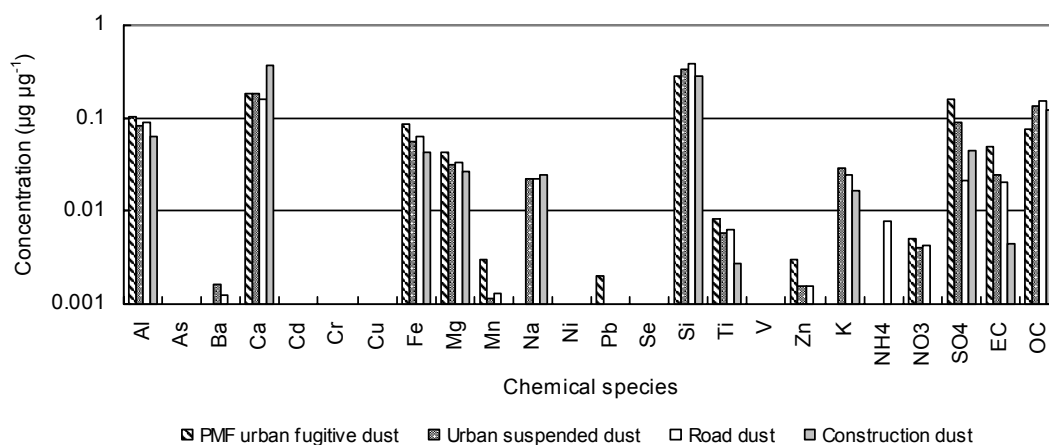
Fig. 5. PMF resolved urban fugitive dust versus three types of measured dust profiles in Beijing.

certain amount of OC, which are characteristics of secondary sulfate. Such pattern has been reported in several PMF studies (Polissar et al., 2001; Kim and Hopke, 2006; Song et al., 2006; Yuan et al., 2006). Secondary sulfate is formed by photochemical reactions, especially in the summer when solar radiation and the ambient temperature are high (Seinfield and Pandis, 1998). The calculated NH_4^+ to SO_4^{2-} molar ratio of 2.1 in the profile indicated that $(NH_4)_2SO_4$, instead of NH_4HSO_4, was the major species formed by SO_4^{2-} and NH_4^+ (Lee et al., 1999; Wang et al., 2005). The presence of OC might be ascribed to that sulfuric acid can catalyze particle-phase heterogeneous reactions of atmospheric organic carbony species when secondary sulfate is formed, resulting in formation of secondary organic aerosols (Jang et al., 2002).

The fifth source profile shown in Fig. 4e contained high concentrations of NO_3^- and NH_4^+ along with certain amount of OC, which were typical characteristics for secondary nitrate. Similar pattern has been reported by Li et al. (2004). NO_x from traffic emission and stationary sources, such as power plants, is oxygenated to HNO_3, and equilibrium between HNO_3 and NH_3 in ambient air leads to the formation of NH_4NO_3. The existence of OC was similar as secondary sulfate and suggested condensation of organic matter on the NH_4NO_3 particles which was consistent with previous studies on individual particles (Liu et al., 2003).

The sixth source profile in Fig. 4f was characterized by high concentrations of OC and K, along with EC, Si, Ca, Fe, Mg, Zn and Pb. OC and K as tracers are commonly used to identify biomass burning (Duan et al., 2004; Song et al., 2006; Lee et al., 2006). OC, EC, Zn, Pb, and K were also identified as signatures for municipal incinerators (Yoo et al., 2002). Therefore this source type was identified as biomass burning with municipal incineration.

The seventh source profile in Fig. 4g was represented by high concentrations of EC and OC, with relatively high concentrations of Zn, Cu, Pb, Ca, Si and Fe. Cadle et al.(1999) found the EC/OC ratio to be 3:7 in gasoline exhaust and 6:4

in desel exhaust. Considering gasoline and diesel accounted for respectively 14.3% and 8.5% of Beijing's total fuel consumption in 2004, and the population of diesel vehicles only accounted for 5% of Beijing's total vehicle population, OC might be much higher than EC for vehicle emission in Beijing. Si, Fe, Zn and Pb have been detected in vehicle emission sources (Cadle et al., 1998). Fe can also be from muffler ablation. Ca is used as lubricating oil additives (Hwang and Hopke, 2006); Cu is emitted from metal brake wear or could be generated from high-volume air sampling pumps (Lee et al., 1999); Si has been linked to heavy-duty diesel emissions (Lee and Hopke, 2006) or is from road dust. Zn has been found to be emitted by motor vehicles (Huang et al., 1994) and has been commonly associated with motor vehicle sources in recent PMF studies. This profile was also quite similar as the vehicle emission source profile for PM$_{2.5}$ in Beijing in 2000 by Song et al. (2006). Therefore, this source should be identified as vehicle emission.

3.3 Temporal trends of ambient PM$_{10}$ source contributions in Beijing in 2004

The daily average mass contributions of each source to ambient PM$_{10}$ in Beijing were calculated by averaging apportionment results at six sites on a daily basis and presented in Fig. 6.

It can be seen in Fig. 6 that the daily average contributions of urban fugitive dust were in the range of 11 to 245 μg m^{-3} and relatively high on all the sampling days. Especially in April, with the daily contributions from 75 μg m^{-3} to 245 μg m^{-3} which were significantly higher than in other months, urban fugitive dust contributed 50.2% of total PM$_{10}$ mass on a monthly basis. According to statistical meteorological data in many years, cyclone and front activities happened frequently in March and April in Beijing and caused the highest frequency of dust weather days in these two months. About 50% of dust weather days on an annual basis
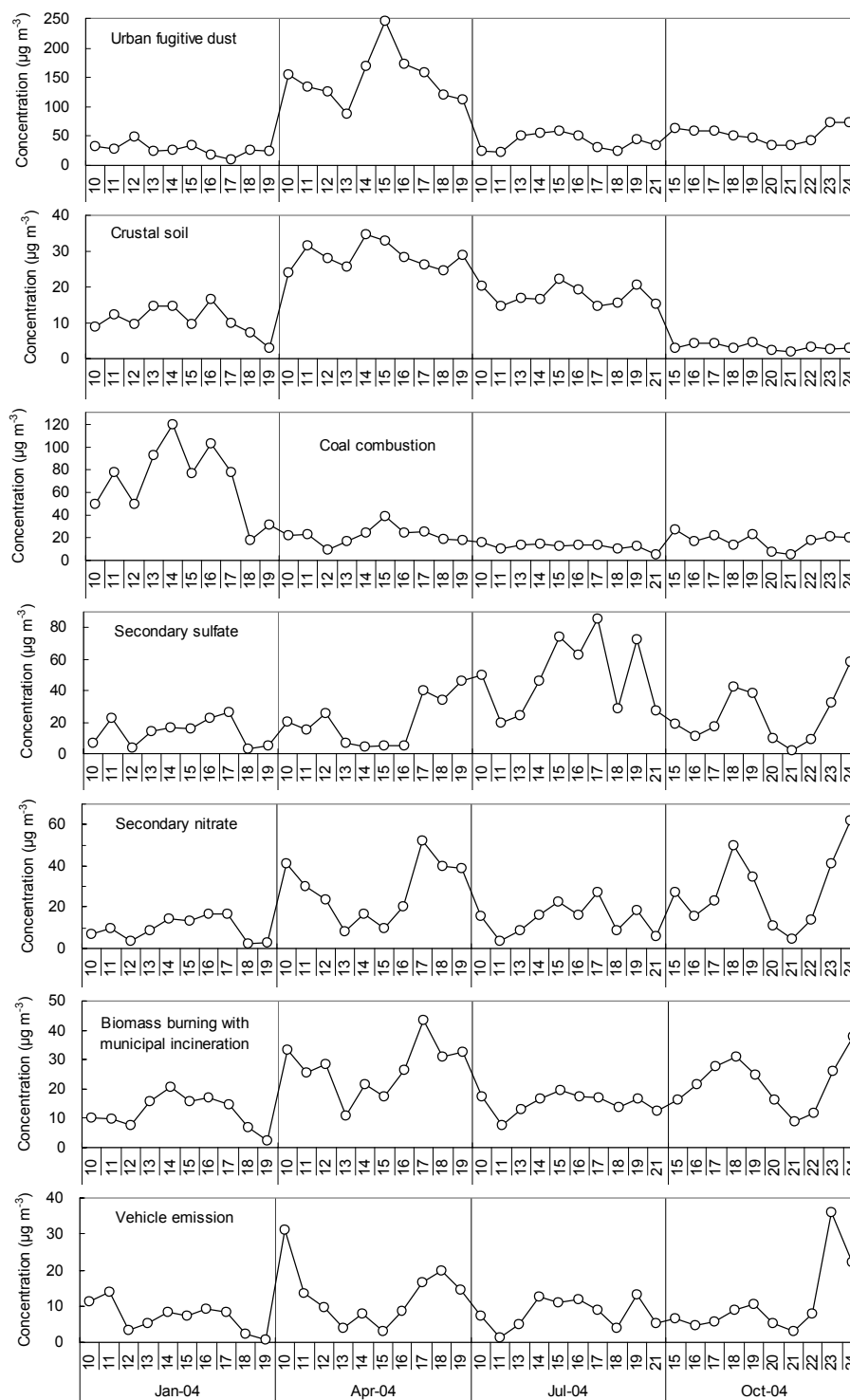
Fig. 6. Daily variations of PM$_{10}$ source contributions in Beijing.

appeared in April, caused by external and internal dust (Xie et al., 2005). On 15 April 2004, strong windy weather dominated in Beijing and the maximum gust speed in the afternoon was as high as 40 mph (www.wunderground.com). As

expected, contribution from urban fugitive dust on this day reached the extremely high concentration of 245.4 μg m^{-3}, reflecting serious local scale resuspended dust pollution. Therefore, the great contribution from urban fugitive dust
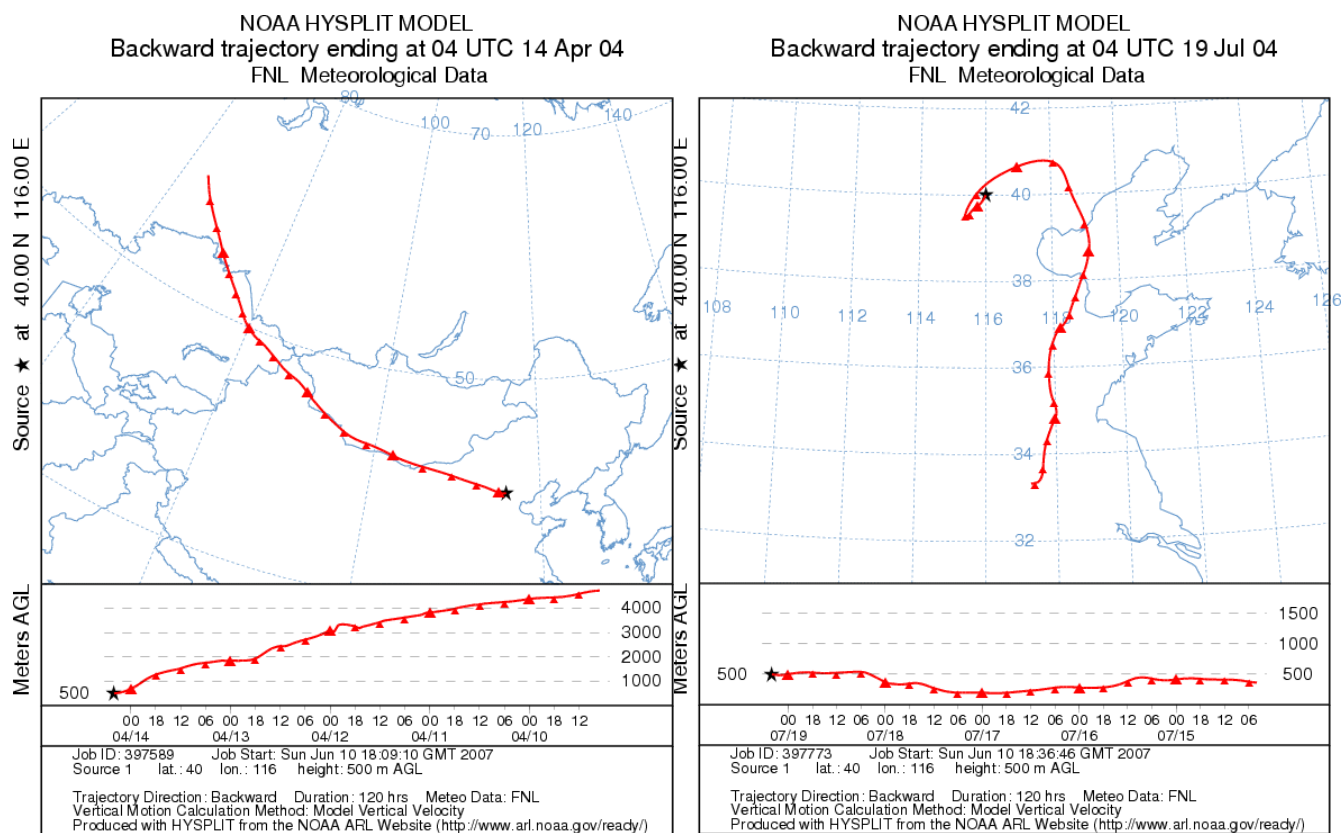
Fig. 7. Backward trajectories arriving at Beijing on April 14 and July 19 in 2004.

in April was due to high wind velocity and indicated high dust loading on the ground surface in Beijing. Oppositely in January, the urban fugitive dust contribution was relatively low as 27.6 μg m^{-3}, accounting for 18.0% of PM$_{10}$ mass concentration due to the cold weather, freezing ground surface, and relatively low dust loading.

By comparing the daily average contributions of urban fugitive dust with those of crustal soil shown in Fig. 6, it was found that the daily average contributions of crustal soil, ranging from 2 to 35 μg m^{-3}, showed a different variation pattern from urban fugitive dust. Monthly average contributions were 10.7 μg m^{-3}, 28.6 μg m^{-3}, 17.7 μg m^{-3} and 3.3 μg m^{-3} for January, April, July, and October, respectively, much lower than those of urban fugitive dust. Crustal soil mainly concentrated in April, followed by July and January. In October, its contribution was almost none.

In order to identify the possilbe transport path for non-local crustal soil to Beijing, backward trajectory ending at Beijing on each sampling day was calculated with NOAA-HYSPLIT model (Draxler and Rolph, 2003). Backward trajectories on 14 April 2004 and 19 July 2004, two typical sampling days with high peak contributions from crustal soil, illustrated in Fig. 7 indicated that non-local dust was from northwest of Beijing on 14 April 2004 and from south of Bei-

jing on 19 July 2004. In addition, downloaded TOMS-NASA global aerosol index maps (TOMS, http://jwocky.gsfc.nasa.gov; Herman et al., 1997) in 2004 exhibited high aerosol concentrations on the northwest of Beijing in April and on the south of Beijing in July, respectively. Oppositely, in October and January, aerosol concentrations in the whole area of China were relatively low. Therefore, it can be concluded that this crustal soil source with high Si and Na concentrations might be mainly from the northwest in April and from the south in July in 2004.

These two dust sources had similar chemical characteristics and were differentiated by PMF, contributing 42.2% of measured total PM$_{10}$ mass concentration, which are consistent with the CMB results by Okuda et al. (2004) in which soil dust accounted for 47% and 42% of PM$_{10}$ concentrations in 2001 and 2002, respectively. By comparing Fig. 3 and Fig. 6, it can be found that PMF identified the different sources for the two high PM$_{10}$ concentration days 14 April 2004 and 15 April 2004. Non-local crustal soil and urban fugitive dust might be the major sources for these two days, respectively, which can be further proved by Fig. 7 and the serious fugitive dust rendered by the great wind whether on 15 April 2004. These also justified our source profiles for these two source.

Table 1. Monthly and annual average PM$_{10}$ source contributions in Beijing, 2004.

Duration	Source contribution	Urban fugitive dust	Crustal soil	Coal combustion	Secondary sulfate	Secondary nitrate	Biomass burning with municipal incineration	Vehicle emission	Unknown
January	μg m^{-3}	27.6	10.7	69.5	13.8	9.5	12.1	7.0	2.8
	%	18.0	7.0	45.4	9.0	6.2	7.9	4.6	1.8
April	μg m^{-3}	147.9	28.6	21.9	20.3	27.9	27.1	12.9	8.4
	%	50.2	9.7	7.4	6.9	9.5	9.2	4.4	2.8
July	μg m^{-3}	39.7	17.7	12.2	49.2	14.6	15.2	8.1	7.6
	%	24.2	10.8	7.4	29.9	8.9	9.2	4.9	4.7
October	μg m^{-3}	53.6	3.3	17.4	24.0	28.4	22.2	11.1	6.4
	%	32.2	2.0	10.4	14.5	17.0	13.3	6.7	3.8
Annual	μg m^{-3}	66.9	15.1	30.0	27.1	20.0	19.1	9.7	6.3
	%	34.4	7.8	15.5	13.9	10.3	9.8	5.0	3.3

Daily average contributions of coal combustion to PM$_{10}$ in 2004 in Beijing showed in Fig. 6 ranged from 5 to 120 μg m^{-3} and displayed a pattern characterized by extremly higher level in January than those in other months. Monthly average contribution in January was 69.5 μg m^{-3}, covering 45.4% of PM$_{10}$ mass concentration, followed by 22 μg m^{-3} in April and 17 μg m^{-3} in October. Due to much less coal consumed in summer, the contribution was only 12 μg m^{-3} in July on a monthly basis. The Daily fluctuations of contributions were great in January but not obvious in other months, which therefore also became an obvious seasonal variation pattern for coal combustion.

Daily contributions from secondary sulfate ranged from 2.6 to 86 μg m^{-3} with high peaks mainly in July. Monthly average contribution was as high as 49.2 μg m^{-3} in July and much higher than in other months, followed by 24.1 μg m^{-3} in October, 20.3 μg m^{-3} in April and 13.8 μg m^{-3} in January. The reason for this pattern is that strong solar radiation, high ambient temperature and relative humidity in July favored the formation of secondary sulfate from SO$_2$ by photochemical reactions (Seinfield and Pandis, 1998). It can be seen in Fig. 6 that daily contributions of secondary sulfate displayed a significant fluctuation, which might be related with the daily variations of meteorological conditions. Specifically, the meteorological data in July 2004 (www.wunderground.com) revealed that the average wind velocities on 13, 14 and 18 July 2004 were in the range of 1.5–2 m s^{-1}, with maximum gust speed of 10–12 m s^{-1}, average temperature of 25–28°C, and moderate rain and thunder shower on 14 and 18 July 2004. These weather constituents went against the formation of secondary sulfate, resulting in the low daily contributions of secondary sulfate. In contrast, fog events, low wind velocity and high ambient temperature occurred on other sampling days in July; such weather constituents were favorable for secondary sulfate formation. Hence, daily contributions of secondary sulfate to PM$_{10}$ reached as high as 85.7 μg m^{-3} on 17 July. The source contribution of secondary sulfate replaced that of urban fugitive dust to become the most in July, with the monthly average contribution of 49.2 μg m^{-3}, accounting for 29.9% of the PM$_{10}$ mass. And the annual average contribution was 27.1 μg m^{-3}, accounting for 13.9% of the total PM$_{10}$ mass.

Daily average contributions from secondary nitrate varied from 2.2 to 62 μg m^{-3} and showed different variation pattern from secondary sulfate, as shown in Fig. 6. Considerable differences for variation ranges were found to exist among sampling days and months, which might depend on different meteorological conditions. The monthly average contributions were 28.4 and 27.9 μg m^{-3} in April and October, while merely 10.3 and 14.6 μg m^{-3} in January and July, respectively. In ambient air, NH$_4$NO$_3$, known as a semi-volatile compound, is the major existence form for NO$_3^-$ and NH$_4^+$. Since low temperature in January does not favor secondary nitrate formation, while high temperature in July leads to decomposition and volatilization of NH$_4$NO$_3$, nitrate concentration were not high in these two months. In contrast, in April and October, high nitrate concentrations were observed due to moderate temperature in these two months. Besides, as seen in Fig. 6, the daily average contributions for secondary nitrate showed similar variation pattern with biomass burning and vehicle emission, which is understandable considering biomass burning and vehicle emission may be sources of NO$_x$, which is an important precursor for secondary nitrate. Therefore, controlling biomass burning and vehicle emission is vital for reducing secondary nitrate contribution in Beijing.

It was seen from the daily contributions of biomass burning with municipal incineration to ambient PM$_{10}$ in 2004 in Fig. 6 that this source contributed in the range from 2.6 to $43\,\mu\mathrm{g\,m}^{-3}$ on a daily basis, and $12.1\,\mu\mathrm{g\,m}^{-3}$ in January, $27.1\,\mu\mathrm{g\,m}^{-3}$ in April, $15.2\,\mu\mathrm{g\,m}^{-3}$ in July and $22.2\,\mu\mathrm{g\,m}^{-3}$ in October, respectively on a monthly basis. Obviously, the daily average contributions in April and October were higher than in other months. The daily contribution variations of this source were smooth in July but considerable in other months, especially in April and July. Furthermore, daily variations for source contributions of biomass burning in April were close to those of urban fugitive dust source. Specifically, it is the right time for spring ploughing in April; wheat straw burning intensifies from May to July; maize straw burning takes place during August through October and fallen leaves are burned during November through next January. PM$_{10}$ emitted by biomass burning source actually exist in all the months around Beijing. Meanwhile, 3–4% wastes in Beijing were incinerated. Therefore their contributions to PM$_{10}$ should not be neglected, which was different from the results of previous PM$_{10}$ source apportionment studies in China (Bi et al., 2005; Okuda et al., 2004). Furthermore, it must be noted that in March and April, apart from local crop burning, non-local biomass burning rendered PM$_{10}$ might be transported to Beijing along with crustal soil, and lead to increase in the daily average contribution of biomass burning and appearing to be similar to the daily variation pattern of daily average contribution of crustal soil and urban fugitive dust in April. Xie et al. (2005) have found that a large quantity of fine particles were transported into Beijing with sand dust during sand-dust storm periods.

The daily average contributions from vehicle emission to PM$_{10}$ in 2004 presented in Fig. 6 showed no obvious fluctuation except on April 10 and October 23. It was seen from Fig. 6 that vehicle emission contributed in the range from 0.6 to $36\,\mu\mathrm{g\,m}^{-3}$ on a daily basis, and $7.0\,\mu\mathrm{g\,m}^{-3}$ in January, $12.9\,\mu\mathrm{g\,m}^{-3}$ in April, $8.1\,\mu\mathrm{g\,m}^{-3}$ in July and $11.1\,\mu\mathrm{g\,m}^{-3}$ in October on a monthly basis. It was a stable source with and the annual average contribution of $9.7\,\mu\mathrm{g\,m}^{-3}$.

3.4 Seasonal and spatial variations of ambient PM$_{10}$ source contributions in Beijing in 2004

Average source contributions on annual and monthly basis were calculated by averaging apportionment results at six sites and shown in Table 1. On average, the contributions from seven sources resolved by PMF accounted for about 96.7% of observed PM$_{10}$ mass concentration. Among them, urban fugitive dust which came from local road traffic, agricultural tilling operations, aggregate storage piles, and heavy construction operations contributed the most in Beijing, with the annual average contribution of $66.9\,\mu\mathrm{g\,m}^{-3}$, accounting for 34.4% of the total PM$_{10}$ mass. The second largest contributor was coal combustion source with contribution of $30.0\,\mu\mathrm{g\,m}^{-3}$, accounting for 15.5% of the total PM$_{10}$ mass

on an annual basis. Contributions of secondary sulfate and secondary nitrate were $27.1\,\mu\mathrm{g\,m}^{-3}$ and $20.0\,\mu\mathrm{g\,m}^{-3}$, accounting for 13.9% and 10.3% of the total PM$_{10}$ mass, respectively, which indicated considerably high contributions of secondary sources to ambient PM$_{10}$ in Beijing. Contribution from biomass burning with municipal incineration was $19.1\,\mu\mathrm{g\,m}^{-3}$, accounting for 9.8% of the total PM$_{10}$ mass. Crustal soil contributed $15.1\,\mu\mathrm{g\,m}^{-3}$, accounting for 7.8% of the total PM$_{10}$ mass. Contribution from vehicle emission was relatively low at $9.7\,\mu\mathrm{g\,m}^{-3}$. However, vehicles not only directly emit particulate matter, but also emit large amount of gaseous pollutants, such as NO$_\mathrm{x}$ and VOC (Cai and Xie, 2007), which will transform to secondary aerosols, including secondary nitrate and organics (Lee and Hopke, 2006; Perrino et al., 2002). In addition, vehicle traveling also causes road dust which is also an important source for PM$_{10}$. Based on this consideration, contribution from vehicles actually accounted for a much larger part than 5.0%. Besides, some existing industrial sources, such as Capital Iron and Steel Company, may be important contributors for iron elements such as Pb, Zn, and Cu, and large source of SO$_2$, which is precursor for secondary sulfate. All these potential sources cannot be neglected either and need more investigation.

It was also found from Table 1 that the contribution of each source to PM$_{10}$ in Beijing showed significant seasonal variations. In January, due to increasing demand for heat supply in winter, coal combustion dominated with the contribution of $69.5\,\mu\mathrm{g\,m}^{-3}$, accounting for 45.4% of total PM$_{10}$ mass. In April, urban and crustal soil became the primary PM$_{10}$ sources. Contribution from urban fugitive dust in this month was as high as $147.9\,\mu\mathrm{g\,m}^{-3}$, accounting for 50.2% of total PM$_{10}$ mass. In July, secondary sources, including secondary sulfate and secondary nitrate, with the contribution of $63.8\,\mu\mathrm{g\,m}^{-3}$, 38.8% were major PM$_{10}$ sources. In October, urban fugitive dust, secondary sulfate and secondary nitrate were the major PM$_{10}$ sources. Contribution from biomass burning in October was also high due to the increase of leaves burned in fall. Overall, urban fugitive dust source contributed large portion of PM$_{10}$ mass concentration in every month and should be the priority to be controlled in Beijing. Monthly average source contributions for each site were illustrated in Fig. 8. It can be seen from Fig. 8 that PM$_{10}$ source contributions in Beijing displayed not only seasonal variations but also spatial differences. The contributions from urban fugitive dust were higher at suburban sites FS, GC, and YZ than at urban sites AT and CGZ. It was indicated that contributions from urban fugitive dust were higher than those from other sources in southeastern and southwestern Beijing, and that dust loading in urban areas was lower than in suburban areas. GC is near Capital Iron and Steel Company, where aggregate storage piles of all kinds of materials might generate suspended dust. Construction materials plants and various roads emitted dust around FS. Coal combustion contributions at AT, CGZ and GC were higher than at other sites. Secondary sulfate and secondary nitrate contributions at AT, CGZ, FS
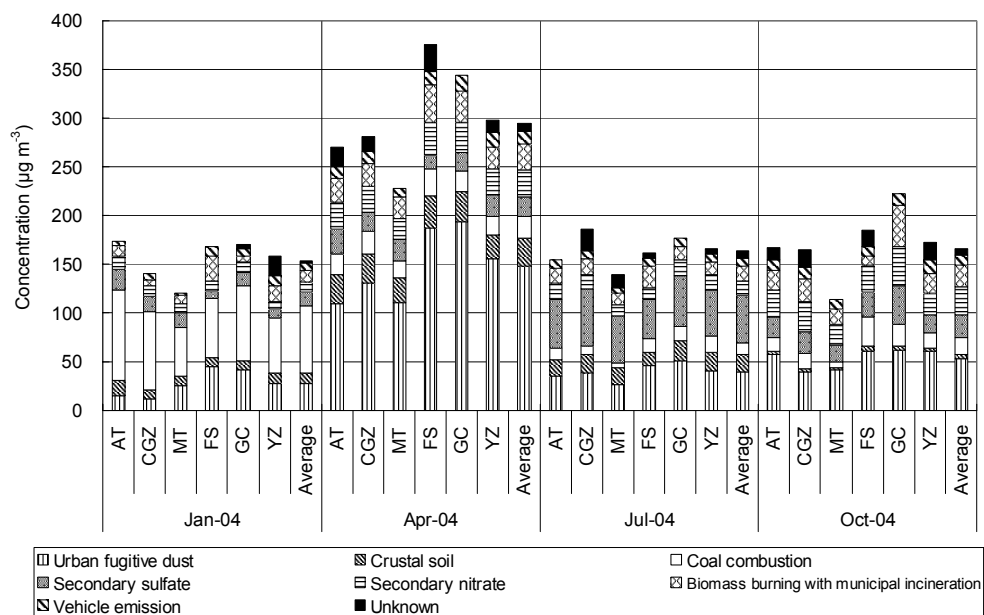
Fig. 8. Monthly average PM$_{10}$ source contributions in January, April, July, and October for each sampling site in Beijing in 2004.

Table 2. Comparison between source contributions for PM$_{10}$ in 2004 and PM$_{2.5}$ in 2000 in Beijing.

	PM$_{10}$ (this study)			PM$_{2.5}$ (Song et al., 2006)	
Resolved source types	Average source contribution		Resolved source types	Average source contribution	
	%	μg m^{-3}		%	μg m^{-3}
Secondary sulfate	13.9	27.1	Secondary sulfate	19.3	18.4
Secondary nitrate	10.3	20	Secondary nitrate	11.6	11.1
Urban fugitive dust	34.4	66.9	Road dust	7.8	7.4
Crustal soil	7.8	15.1	Yellow dust	4.9	4.7
Biomass burning with municipal incineration	9.8	19.1	Biomass burning	9.8	9.4
Coal combustion	15.5	30	Coal combustion	17.2	16.4
Vehicle emission	5	9.7	Vehicle emission	5.9	5.6
			Industry	5.6	5.3
Unknown	3.3	6.3	Unknown	17.9	17.1

and GC were higher than at other two sites. Biomass burning contribution at FS was much higher than at other sites. This was probably due to biomass burning activities in kilns around FS or transported PM$_{10}$ from the southwest, considering FS was located on the southwestern transport path in Beijing.

Sums of PMF resolved source contributions on all the sampling days and sites were calculated to represent the reconstructed PM$_{10}$ mass concentrations. And then reconstructed versus observed PM$_{10}$ mass concentrations were plotted. As seen in Fig. 9, reconstructed PM$_{10}$ concentrations showed good agreements with observed values, with a R^2=0.92, a lope 0.92 and an intercept 8.93 μg m^{-3}. These indicated a successful source apportionment and credible results.

In Table 2, PM$_{10}$ souce contritutions in 2004 and PM$_{2.5}$ source contributions in 2000 (Song et al., 2006) in Beijing were compared. 8 and 7 sources were identified for PM$_{2.5}$ in 2000 and for PM$_{10}$ in 2004, respectively. Different from PM$_{2.5}$ in 2000, industial source was not identified for PM$_{10}$ but municipal incineration was found, which agreed well with the facts in Beijing: industries were ordered to move outside Beijing from 1999 and waste incineration plants began to be under construction from 2003. Meanwhile, the particle size characteristics for different emission sources can be found in Table 2, although based on data in different years. Secondary sulfate, secondary nitrate, biomass burning with municipal incineration and vehicle emission mainly emitted PM$_{2.5}$, urban fugitive dust and crustal soil were mainly
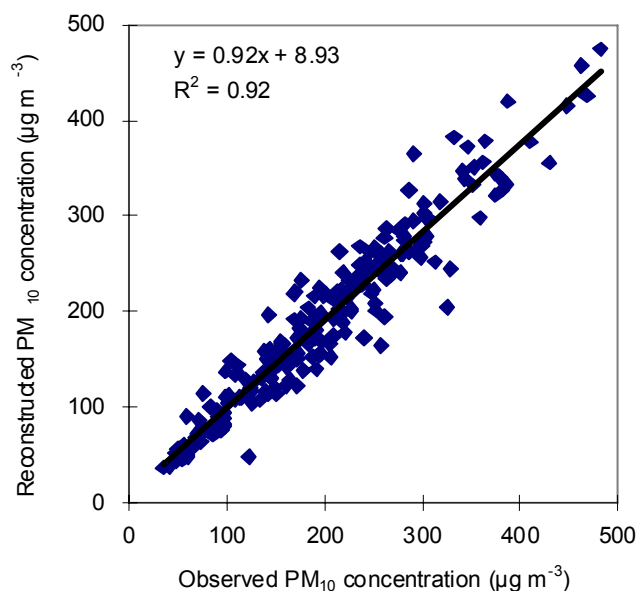
$$y = 0.92x + 8.93$$
$$R^2 = 0.92$$

Fig. 9. Observed versus reconstructed PM$_{10}$ mass concentrations.

comprised of larger particles, and coal combustion emitted particles with both sizes.

4   Conclusions

The average PM$_{10}$ concentration in Beijing during the sampling period in 2004 was 194 μg m^{-3}, which exceeded National Ambient Air Quality Standard (GB3095-1996) level II for PM$_{10}$ (100 μg m^{-3}) and also exceeded level III (150 μg m^{-3}). PM$_{10}$ in Beijing was mainly composed of crustal elements, organic matter, SO$_4^{2-}$ and NO$_3^-$, which accounted for 8.6%, 39.9%, 16.1% and 13.5% of total PM$_{10}$ mass on an annual basis. Crustal elements accounted for more than 40% of PM$_{10}$ mass concentration in January, April, and July. SO$_4^{2-}$ accounted for 26.9% in July and NO$_3^-$ accounted for 14.1% of PM$_{10}$ mass concentration in October, both of which were significantly higher than in other months.

Seven sources of ambient PM$_{10}$ in Beijing in 2004 were resolved by PMF, which were urban fugitive dust, crustal soil, coal combustion, secondary sulfate, secondary nitrate, biomass burning with municipal incineration and vehicle emission. In paticular, urban fugitive dust and crustal soil as two types of dust sources with similar chemical characteristics were differentiated by PMF. Urban fugitive dust was the largest contributor with the annual average contribution of 66.9 μg m^{-3}, accounting for 34.4% of PM$_{10}$ mass concentration. Coal combustion was still an important source of PM$_{10}$ in Beijing. Especially in winter, its contribution reached 69.5 μg m^{-3}, accounting for 45.4% of the total PM$_{10}$ mass. Secondary sources including secondary sulfate and secondary nitrate contributed 47.1 μg m^{-3}, accounting for 24.3% of the total PM$_{10}$ mass, indicating quite serious

secondary pollution in Beijing. Contributions of biomass burning and vehicle emission were 19.1 μg m^{-3}, 9.8% and 9.7 μg m^{-3}, 5.0%, respectively. In spite of the relative low contribution from direct vehicle emission, considering secondary aerosols formed by oxidation of vehicles emitted gaseous precursors and resuspended dust caused by vehicle traveling, PM$_{10}$ generated by vehicles, both directly and indirectly, were quite significant and should not be neglected.

The source apportionment results of ambient PM$_{10}$ in 2004 in Beijing indicated that significant seasonal and spatial variations of PM$_{10}$ sources in Beijing were found. Coal combustion was the primary source of ambient PM$_{10}$ in winter which accounted for 45.4% of PM$_{10}$ mass concentration. Higher contributions were found in urban areas than in suburban areas. Urban fugitive dust contributed 50.2% of PM$_{10}$ mass concentration in spring, and was significant in other months, too. Higher contributions from urban fugitive dust were found in southwestern and southeastern suburban areas than in central urban areas, indicating higher dust loadings in these areas. Secondary sulfate and secondary nitrate combined to be the largest source in summer and fall, with percentages of 38.8% and 31.5%, respectively. Contributions from secondary sources were higher in urban areas than in suburban areas. Biomass burning with municipal incineration contributed more in fall than in other months, and more in southwestern Beijing than in other areas, which indicated biomass burning with municipal incineration sources might locate in southwestern area of Beijing. In conclusion, it was found that ambient PM$_{10}$ sources in Beijing showed significant seasonal variations as well as spatial differences.

References

Beijing Environmental Protection Bureau: Report on the State of the Environment in Beijing in 2002, www.bjepb.gov.cn/bjhb/tabid/68/InfoID/2618/Default.aspx, 2004.

Beijing Environmental Protection Bureau: Report on the State of the Environment in Beijing in 2004, www.bjepb.gov.cn/bjhb/tabid/68/InfoID/2620/Default.aspx, 2005.

Beijing Environmental Protection Bureau: Report on the State of the Environment in Beijing in 2005, www.bjepb.gov.cn/bjhb/tabid/68/InfoID/7622/Default.aspx, 2006.

Bi, X., Feng, Y., Wu, J., Wang, Y., and Zhu, T.: Source apportionment of PM$_{10}$ in six cities of northern China, Atmos. Environ., 41, 903–912, 2007.

Cadle, S. H., Mulawa, P., Hunsanger, E. C., Nelson, K., Ragazzi, R. A., Barrett, R., Gallagher, G. L., Lawson, D. R., Knapp, K.

T., and Snow, R.: Measurements of exhaust particulate matter emissions from in-use light-duty motor vehicles in the Denver, Colorado area, report prepared for coordinating research council, Atlanta GA, 1998.

Cadle S. H., Mulawa P. A., Hunsanger E. C., Nelson K, Ragazzi R. A., Barrett R., Gallagher G. L., Lawson D. R., Knapp K. T., and Snow R.: Composition of light-duty motor vehicle exhaust particulate matter in the Denver, Colorado area, Environ. Sci. Technol., 33, 2328–2339, 1999.

Cai, H. and Xie, S. D.: Estimation of vehicular emission inventories in China from 1980 to 2005, Atmos. Environ., doi:10.1016/j.atmosenv.2007.08.019, 2007.

Chen, T., Hua, L., Jin, L., Xu, Z., Wang, H., Bai, J., Liu, W., Hu, Y., and Lin, A.: Research on PM$_{10}$ source apportionment in Beijing, Environmental Monitoring in China, 22, 6 (in Chinese with abstract in English), 2006.

Christoforou, C. S., Salmon, L. G., Hannigan, M. P., Solomon, P. A., Cass, and G. R.: Trends in fine particle concentration and chemical composition in southern California, J. Air Waste Manag. Assoc., 50, 43–53, 2000.

Draxler, R. R. and Rolph, G. D.: HYSPLIT (HYbrid Single-Particle Lagrangian Integrated Trajectory) model access via NOAA ARL READY Website, www.arl.noaa.gov/ready/hysplit4.html, 2003.

Duan, F., Liu, X., Yu, T., and Cachier, H.: Identification and estimate of biomass burning contribution to the urban aerosolorganic carbon concentrations in Beijing, Atmos. Environ., 38, 1275–1282, 2004.

Han, J. S., Moon, K. J., Lee, S. J., Kim, Y. J., Ryu, S. Y., Cliff, S. S., and Yi, S. M.: Size-resolved source apportionment of ambient particles by positive matrix factorization, Atmos. Chem. Phys., 6, 211–223, 2006,
http://www.atmos-chem-phys.net/6/211/2006/.

Hedberg, E., Gidhagen, L., and Johansson, C.: Source contributions to PM$_{10}$ and arsenic concentrations in Central Chile using positive matrix factorization. Atmos. Environ., 39, 549–561, 2005.

Hopke, P. K., Lamb, R. E., and Natusch, D. F. C.: Multi-elemental characterization of urban roadway dust, Environ. Sci. Technol., 14, 164–172, 1980.

Hua, L., Guo, J., Xu, Z., Hu, Y., Huang, Y., and Zou, B.: Analysis of PM$_{10}$ source profiles in Beijing. Environmental Monitoring in China 22, 6, 64–71 (in Chinese with abstract in English), 2006.

Huang, X. D., Olmez, I., Aras, N. K., and Gordon, G. E.: Emissions of trace-elements from motor-vehicles-potential marker elements and source composition profile, Atmos. Environ., 28, 1385–1391, 1994.

Hwang, I. and Hopke, P. K.: Comparison of source apportionments of fine particulate matter at two San Jose Speciation Trends Network Sites, J. Air Waste Manag. Assoc., 56, 1287–1300, 2006.

Jang, M., Czoschke, N. M., Lee, S., and Kamens, R. M.: Heterogeneous atmospheric aerosol production by acidcatalyzed particle-phase reactions, Science, 298, 814–817, 2002.

Johnson, K. S., de Foy, B., Zuberi, B., Molina, L. T., Molina, M. J., Xie, Y., Laskin, A., and Shutthanandan, V.: Aerosol composition and source apportionment in the Mexico Metropolictan Area with PIXE/PESA/STIM and multivariate analysis, Atmos. Chem. Phys., 6, 4591–4600, 2006,
http://www.atmos-chem-phys.net/6/4591/2006/.

Kim, E. and Hopke, P. K.: Characterization of fine particle sources in the Great Smoky Mountains area, Sci. Total Environ., 368, 781–794, 2006.

Lanz, V. A., Alfarra, M. R., Baltensperger, U., Buchmann, B., Hueglin, C., and Prévot A. S. H.: Source apportionment of submicron organic aerosols at an urban site by factor analytical modeling of aerosol mass spectra, Atmos. Chem. Phys., 7, 1503–1522, 2007,
http://www.atmos-chem-phys.net/7/1503/2007/.

Li, Z., Hopke, P. K., Husain, L., Qureshi, S., Dutkiewicz, V. A., Schwab, J. J., Drewnick, F., and Demerjian, K. L.: Sources of fine particle composition in New York city, Atmos. Environ., 38, 6521–6529, 2004.

Lee, E., Chan, C. K., and Paatero, P.: Application of positive matrix factorization in source apportionment of particle pollutants in Hong Kong, Atmos. Environ., 33, 3201–3212, 1999.

Lee, P. K. H., Brook, J. R., Zlotorzynska, E. D., and Mabury, S. A.: Indentification of the major sources contributing to PM$_{2.5}$ observed in Toronto, Environ. Sci. Technol., 37, 4831–4840, 2003.

Lee, J. H. and Hopke, P. K.: Apportioning sources of PM$_{2.5}$ in St. Louis, MO using speciation trends network data, Atmos. Environ., 40, 360–377, 2006.

Liu, W., Hopke, P. K., Han, Y. J., Yi, S. M., Holsen, T. M., Cybart, S., Kozlowski, K., and Milligan, M.: Application of receptor modeling to atmospheric constituents at Potsdam and Stockton, NY, Atmos. Environ., 37, 4997–5007, 2003.

Okuda, T., Kato, J., Mori, J., Tenmoku, M., Suda, Y., Tanaka, S., He, K., Ma, Y., Yang, F., Yu, X., and Duan, F.: Daily concentrations of trace metals in aerosols in Beijing, China, determined by using inductively coupled plasma mass spectrometry equipped with laser ablation analysis, and source identification of aerosols, Sci. Total Environ. 330, 145–158, 2004.

Paatero, P.: User's guide for positive matrix factorization programs PMF2 and PMF3, Part 1: tutorial, 2004.

Paatero, P. and Tapper, U.: Positive matrix factorization: a non-negative factor model with optimal utilization of error estimates of data values, Environmetrics, 5, 111–126, 1994.

Paatero, P.: Lest squares formulation of robust non-negative factor analysis, Chemometr. Intell. Lab., 37, 23–35, 1997.

Perrino, C., Catrambone, M., Di Menno Di Bucchianico, A., and Allegrini, I.: Gaseous ammonia in the urban area of Rome, Italy and its relationship with traffic emissions, Atmos. Environ., 36, 5385–5394, 2002.

Polissar, A. V., Hopke, P. K., and Poirot, R. L.: Atmospheric aerosolover Vermont: chemical composition and sources, Environ. Sci. Technol., 35, 4604–4621, 2001.

Polissar, A. V., Hopke, P. K., Paatero, P., Malm, W. C., and Sisler, J. F.: Atmospheric aerosol over Alaska, 2. Elemental composition and sources, J. Geophys. Res., 103, 19 045–19 057, 1998.

Reff, A, Eberly, S. I., and Bhave, P. V.: Receptor modeling of ambient particulate matter data using positive matrix factorization: Review of exising methods, J. Air Waste Manag. Assoc., 57, 146–154, 2007.

Seinfeld, J. H. and Pandis, S. N.: Atmospheric Chemistry and Physics from Air Pollution to Climate Change, Wiley, New York, USA, 649–655, 1998.

Song, Y., Zhang, Y., Xie, S.D., Zeng, L., Zheng, M., Salmon, L. G., Shao, M., and Slanina, S.: Source apportionment of PM$_{2.5}$ in Beijing by positive matrix factorization, Atmos. Environ., 40, 1526–1537, 2006.

Song, Y., Tang, X., Xie, S. D., Zhang, Y., Wei, Y., Zhang, M., Zeng, L., and Lu, S.: Source apportionment of PM$_{2.5}$ in Beijing in 2004, J. Hazard. Mater., 146, 124–130, 2007.

State Environmental Protection Administration: Report on the State of the Environment in China, www.zhb.gov.cn/ztbd/sjhjr/2007hjr/tpbd56/200706/P020070611461716557487.pdf, 2005.

State Environmental Protection Administration: Report on the State of the Environment in China, www.zhb.gov.cn/download/2004gb.pdf, 2007.

Sun, Y., Zhuang, G., Wang, Y., Han, L., Guo, J., Dan, M., Zhang, W., Wang, Z., and Hao, Z.: The air-borne particulate pollution in Beijing – concentration, composition, distribution and sources, Atmos. Environ., 38, 5991–6004, 2004.

Wang, M.: Study on sources of aerosol in Beijing using factor analysis, Chinese J. Atmos. Sc., 9, 73–81, 1985.

Wang, Y., Zhuang, G., Tang, A., Yuan, H., Sun, Y., Chen, S., and Zheng, A.: The ion chemistry and the source of PM$_{2.5}$ aerosol in Beijing, Atmos. Environ., 39, 3771–3784, 2005.

Xie, S. D., Yu, T., Zhang, Y. H., Zeng, L. M., Qi, L., and Tang, X. Y: Characteristics of PM$_{10}$, SO$_2$, NO$_x$ and O$_3$ in ambient air during the dust-storm period in Beijing, Sci. Total Environ., 345, 153–164, 2005.

Yoo, J. I., Kim, K. H., Jang, H. N., Seo, Y. C., Seok, K. S., Hong, J. H., and Jang, M.: Emission characteristics of particulate matter and heavy metals from small incinerators and boilers, Atmos. Environ., 36, 5057–5066, 2002.

Yuan, Z., Yu, J. Z., Lau, A. K. H., Louie, P. K. K., and Fung, J. C. H.: Application of positive matrix factorization in estimating aerosol secondary organic carbon in Hong Kong and its relationship with secondary sulfate, Atmos. Chem. Phys., 6, 25–34, 2006, http://www.atmos-chem-phys.net/6/25/2006/.

Zabalza, J., Ogulei, D., Hopke, P. K., Lee, J. H., Hwang, I., Querol, X., Alastuey, A., and Santamaria, J. M: Concentration and sources of PM$_{10}$ and its constituents in Alsasua, Spain, Water Air Soil Poll., 174, 385–404, 2006.

Zheng, M., Salmon, L. G., Schauer, J. J., Zeng, L., Kiang, C. S., Zhang, Y., and Cass, G. R.: Seasonal trends in PM$_{2.5}$ source contributions in Beijing, China, Atmos. Environ., 39, 3967–3976, 2005.